Dynamic particle-surface tribocharging: The role of shape and contact mode

Peter M. Ireland
Centre for Advanced Particle Processing /
Discipline of Chemical Engineering
University of Newcastle, Australia
Phone: +61 (0) 2 4921 6181
E-mail: Peter.Ireland@newcastle.edu.au

***Abstract*—Triboelectric charging of particles is exploited in a variety of industrial processes, such as electrophotographic toner charging and triboelectric separation. Dynamic particle-surface contact is a key charging mechanism in many types of particle tribocharger (e.g. cyclones, slides and baffled drop columns), and has therefore been studied in some detail. Models of dynamic charging have tended to assume that the particle is spherical, but this is rarely the case in practice. Experiments have shown that particle shape can strongly influence the charging behaviour via both the mean contact area and the time-varying character of the contact. We review some of the experimental work, then present a 2D model of the dynamic contact of an elliptical particle, of varying roundness ratio, with a flat surface. It incorporates a simple sub-model of the cumulative surface charge transfer. This model captures a rich variety of contact modes not exhibited by spherical particles, including sliding, rolling, tumbling and bouncing. All of these contact modes produce very different charge transfer and accumulation behaviours, and these are studied and compared.**

I. INTRODUCTION

Triboelectrification is a ubiquitous feature of many dry particulate systems [1-3]. It can manifest itself in a variety of ways, including adhesion to vessels or pipe walls [4], changes in dispersion or aggregation behaviour [5, 6], or discharges, leading to significant explosion hazards in dry powder systems [7]. Tribocharging of particulates can also be exploited in processes such as photocopier toner handling [8] and dry triboelectric separation [3, 9-13]. In the latter process, the components of a mixed particulate are given different charges by contact or friction. The components are then separated by passing the differentially-charged mixture through an electric field.

Contact interactions in particle processing systems can occur either between particles or between a particle and another object, usually the vessel or conduit wall [14]. This paper deals with the second of these mechanisms. It is well known that the mechanical nature of the interaction between a particle and a solid surface strongly influences the exchange of

charge. For instance, tribocharging tends to increase with the interaction energy, and sliding contact tends to transfer more charge than simple normal contact [2]. The reasons for these trends are usually multiple and complex. Charge exchange during single particle-surface impacts has previously been studied in some detail [15-20], and some attention has also been paid to the exchange of charge between a continuous flow of particulate material and a solid surface [21, 22]. Both formal studies and anecdotal accounts from industry agree that the broad 'character' of the particle-surface contact has a strong effect on the exchange of charge. The present author has been advised on a number of occasions by industrial practitioners that some tribochargers are only effective if the particles can be made to 'slide' on the tribocharging surface. These accounts raise as many questions as they answer - for instance, in this context, what exactly constitutes 'sliding'? Is continuous contact the most important factor, or is the presence of slip, as opposed to rolling, more important? As another example, pneumatic cyclones represent a very effective means of tribocharging coarse mineral particulates prior to separation, e.g. [23, 24]. Measurements of charge transfer in cyclones suggest qualitative differences in charging behaviour for different modes of contact (i.e. sliding, rolling or bouncing) between the particles and the inside of the cyclone [25]. The operation and design of cyclone tribochargers need to be informed by these considerations if they are to be used effectively. Similar considerations also govern the design and operation of other types of tribocharger [26], and of conveying systems where triboelectric effects are important.

Formal studies of sliding particulate charging on flat surfaces [21, 22] have begun to answer these questions. In these studies, the mode of particle-surface contact was observed closely, using high-speed video footage, as the particles travelled down a flat tribocharging chute. These observations were compared with measurements of the resulting charge. Quantitative characterisation of the contact mode was provided by measuring the instantaneous fraction of particles in contact with the surface, the proportion of particles that were in continuous contact with the surface, and the proportion that were rolling during contact (as opposed to maintaining a fixed orientation). It was confirmed that the time the particles spent in actual contact with the surface (as distinct from the time they took to traverse the chute) was an important determinant of the transferred charge, as expected. Since contact time was in turn determined by whether the particles bounced on the surface (as opposed to rolling or sliding), the presence or absence of bouncing was clearly critical to determining the charge. On the other hand, one would expect the instantaneous normal force during contact, and thus the contact area, to be larger for bouncing than for continuous rolling or sliding. There was also some evidence that the very fact of non-continuous contact somehow limited the charge, perhaps due to gas breakdown discharge during separation of the particles from the surface [16, 17]. Apart from these two factors, it was concluded that the distinction between rolling and fixed-orientation contact was critical to the charge transfer. A rolling particle progressively makes its entire accessible surface area available for charging, whereas a particle that slides with a fixed orientation only presents a limited portion of its surface for charging. On the other hand, assuming that the particle is non-spherical, the average instantaneous contact area for fixed-orientation sliding will tend to be larger than the average contact area for rolling, since the most stable fixed orientations will tend to be those that present the least curved part of the particle to the charging surface. Given the multiplicity of possible factors affecting the

charge transfer, it is hardly surprising that these studies were unable to definitively determine the contribution of each, nor answer several other important questions regarding the charging process. For instance, no light was shed on the age-old question of whether sliding contact is inherently different to static contact in this context.

The studies discussed above strongly reinforced the importance of particle shape. The shape directly determines the contact area and pressure, and is also one of the key factors affecting the contact mode (rolling, sliding, bouncing, tumbling), thereby also having a strong indirect effect on the contact time, force and area. The model developed in [22, 27] incorporated only a crude estimate of the average contact area for a rolling irregularly-shaped particle. Furthermore, no attempt was made to understand the effect of varying particle geometry on contact mode.

In this paper, we attempt to understand the effect of particle geometry on dynamic particle-surface tribocharging a little better by modelling a rather idealised system whose behaviour depends on a relatively small number of dimensionless variables. By initially exploring particle charge behaviour in this deliberately limited parameter space, we hope to develop a structure around which to build more sophisticated and realistic models in the future. The present model is two-dimensional, and the particle shape is restricted to an ellipse of varying roundness ratio. The simplest available models of elastic and inelastic contact (including friction) between the particle and the surface are used to calculate the linear and rotational motion of the ellipse. Two separate charge transfer models are used. In both cases, the particle is assumed to be a perfect insulator, and the flat surface a perfect conductor. The first is a simple capacitive static contact model. The second is slightly more complex, and includes a frictional charging term. It is important to provide a disclaimer at the outset: this frictional charging component has not been physically validated for any real system. It is designed to be as simple as possible, and broadly physically plausible. The same disclaimer applies to the model as a whole. At this stage, its purpose is illustrative and exploratory rather than predictive - a useful tool for gaining physical insight rather than a definitive quantitative model.

II. MODEL

A. Particle motion

The model particle is an ellipse, long axis $2a$ and short axis $2b$. The 'roundness ratio' $\varepsilon\ (\equiv b/a)$, the reciprocal of the aspect ratio, is the main means of characterising the particle geometry. Two sets of coordinates are used; the unprimed coordinates (x,y) refer to the directions tangential and normal to the flat surface, and the primed coordinates (x',y') are external horizontal and vertical coordinates, as shown in Fig. 1. The position of the centre of the ellipse is denoted (x_0,y_0). The angle between these systems (the tilt of the surface) is β. The anticlockwise angle between the long axis of the ellipse and the surface is denoted ϕ, and the anticlockwise angle formed by the contact point, the ellipse centre and the long axis is denoted θ, as shown. The distance from the ellipse centre to the contact point is r, and the local radius of curvature of the ellipse surface at the contact point is r_c. The geometric relationships between these lengths and angles are given in the *Appendix*.

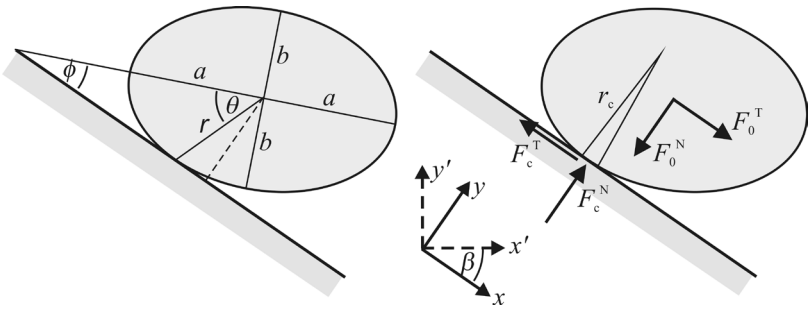

Fig. 1. Schematic of a two-dimensional elliptical particle in contact with a tilted surface, showing the coordinate axes, the important geometric quantities, and the forces on the particle.

The component of the external force on the particle tangential to the surface is denoted F_0^{T}, while the normal component is denoted F_0^{N}. Similarly, the tangential component of the contact force is $F_{\mathrm{c}}^{\mathrm{T}}$, and the normal component is $F_{\mathrm{c}}^{\mathrm{N}}$. Note that the direction of the arrows in Fig. 1 is that of the typical force vector in each case; F_0^{N} and $F_{\mathrm{c}}^{\mathrm{T}}$ as shown would have negative numerical values in the present coordinate system. For all of the simulations performed here, the external force on the particle is assumed to be due to gravity, and to act in the negative-y' direction. In this case,

$$F_0^{\mathrm{T}} = mg\sin\beta\,;\; F_0^{\mathrm{N}} = -mg\cos\beta\ . \tag{1}$$

For elastic deformation, the normal contact force between an infinite cylinder and a half-space (the 2D analogue of Hertzian indentation by a sphere) is proportional to the indentation distance, and is independent of the curvature of the indenting body [27]. We use this to approximate the contact relationship for an elliptical particle. $F_{\mathrm{c}}^{\mathrm{N}}$ is therefore given by the indentation distance d_{y} (calculated in the *Appendix*) multiplied by an elastic constant k. It also includes a dissipative term to allow for energy loss during collisions with a strong normal component; this component is assumed proportional to the elastic component of the normal force, but its direction is always opposite to the normal velocity of the particle (while in contact). The proportionality constant is denoted v.

$F_{\mathrm{c}}^{\mathrm{T}}$ is calculated using a slip-stick-roll model. Coulomb friction is assumed at the interface, and for simplicity, static and kinetic friction coefficients are assigned the same value, μ. For small lateral elastic displacements, $F_{\mathrm{c}}^{\mathrm{T}}$ is assumed proportional to the tangential sticking compliance d_{x}, which takes into account rolling and subsequent sliding (calculated in the *Appendix*). For simplicity, the same elastic constant, k, is used as for normal

contact. The largest value F_c^T can take is the Coulomb limit, i.e. μF_c^N, and slip occurs if this limit is exceeded. Of course, this friction force always opposes the direction of slip (although not necessarily direction of linear motion of the particle.) As explained in the *Appendix*, the elastic compliance is updated for slipping and rolling, and re-stick following a period of sliding is entirely possible. Full equations for the various force components, and the resulting equations of motion, are given in the *Appendix* in both dimensional and dimensionless form, using the dimensionless variables in Table 1.

TABLE 1: DIMENSIONLESS VARIABLES - PARTICLE MOTION

Variable	=
X_0, Y_0	x_0 / a , y_0 / a
τ	$t\sqrt{k/m}$
Ψ	$F/(ka)$
ε	b/a
Γ	$mg/(ka)$
ρ	r/a
ρ_c	r_c / a
δ_x, δ_y	d_x / a , d_y / a

Apart from the initial velocity, position and orientation of the particle, the key parameters governing the dynamics of the particle are ε, Γ, and the two dissipative coefficients, μ and ν. The equations of motion were solved using a Runge-Kutta-Nyström scheme with a step size $\Delta\tau = 8\times10^{-5}$. In this paper, Γ is given a constant value of 0.001, the plane is kept at a tilt of 45°, and we set $\mu = \nu$. The two parameters explored are therefore the particle roundness ratio and a generic dissipation (i.e. friction) coefficient.
It is important to note that the model as a whole ignores the effect of electrostatic forces on the particle motion. These simulations are assumed to take place in a regime where the electrostatic forces are insignificant compared to the gravitational and elastic forces.

B. Static charge transfer

Our first charging model assumes that there is no qualitative difference between static and sliding contact. It does not require a distinction to be made between actual and apparent contact areas. Contact charging systems are frequently modelled by drawing an analogy with charge build-up on a capacitor. We assume that the flat plate is an earthed conductor, thereby ensuring that the charge distribution on its surface during contact is the image of that on the particle. Under these circumstances, the instantaneous charge transfer rate be-

tween a region of the particle surface with charge surface density σ and the conducting plate will be

$$\frac{d\sigma}{dt_c} = \frac{1}{t_0}(\sigma_0 - \sigma) \quad , \tag{2}$$

where t_0 is the characteristic charging time, and σ_0 is the saturated charge density, proportional to the electrochemical potential difference between the two materials [28]. Note that t_c is the time the particle spends in contact with the plate, and does not include any time it may spend in the air during bouncing or tumbling contact. The charge transfer to or from the particle surface is assumed to be governed by Eq. (2) at points in contact with the plane, and zero elsewhere. According to [27], when a body of curvature r_c indents into an elastic half-space to a depth d_y (in two dimensions), the contact half-width is given by

$$s_c = \sqrt{r_c d_y} \quad , \tag{3}$$

or in dimensionless form,

$$S_c = \sqrt{\rho_c \delta_y} \quad . \tag{4}$$

In our model, the particle boundary was separated into 2000 segments of equal arc-length. For each time-step, charge was allowed to build up in the manner indicated by (2), on those segments within a surface distance S_c of the centre of contact during that time-step.

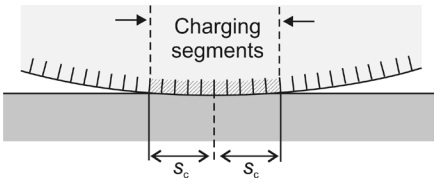

Fig. 2. Model contact between the particle and the plate. Charge is only transferred to those boundary segments that are in contact with the plate at any given time.

This is illustrated in Fig. 2; it is understood that the indentation distance is much smaller than the radius of curvature of the particle surface, as shown. Since the particle was assumed to be an insulator, charge was not permitted to flow laterally between these surface segments.

We have treated the interface as if the apparent contact area and the actual, microscopic contact area are equivalent (or at least, that the actual contact area as a proportion of the apparent contact area is constant). In reality, the actual contact area for a given apparent

contact area will vary with the normal pressure [29], an assumption implicit in the Coulomb friction model, among other things. In a real indentation system with the geometry shown in Figure 2, the contact pressure would be maximum at the centre and would drop off to zero at the edge, as would the actual contact area per unit apparent area. These subtleties are reserved for a more sophisticated model.

C. Sliding charge transfer

The primary obstacle to inclusion of sliding triboelectrification into our model is the mysterious and complex nature of the process, which occurs to a different extent (and even polarity) for different systems and dynamic regimes [30-33]. In choosing a sliding triboelectrification model for illustrative purposes, simplicity and physical plausibility are preferred to validation in any specific system. In our model, a constant (relatively small) fraction of the work done by friction goes into increasing the contact potential difference, and ultimately into 'pushing' more charge across the interface. Lowell [34] put forward a 'molecular stirring' or 'redistribution layer' mechanism (in the context of polymer charging) that may be consistent with this model. In this process, 'full' charge carriers near the surface are mechanically 'ploughed' deeper into the material by friction at the interface, and replaced by 'empty' ones brought up from the bulk. For the moment, though, we do not favour any specific physical mechanism, and merely assume the aforementioned link between frictional work and contact potential difference. Since there is no physical evidence for this model, it should be considered entirely provisional, to be replaced when a better-validated model is developed. Consider an interface for which the saturated surface density of the transferred charge during static contact is σ_0, as in Eq. (2). Let the effective capacitance per unit area of the interface be a constant, κ. The energy density for static contact will therefore be

$$\frac{E_0}{A} = \frac{1}{2}\kappa {V_0}^2 = \frac{1}{2}\frac{{\sigma_0}^2}{\kappa} \quad , \tag{5}$$

where V_0 is the contact potential difference for static contact and A is the interface area. We now assume that work W is done by sliding friction at the interface, and that a constant fraction η of this goes into increasing the dynamic saturation charge density σ_s. Eq. (5) implies that

$$\frac{1}{2}\frac{{\sigma_s}^2}{\kappa} = \frac{1}{2}\frac{{\sigma_0}^2}{\kappa} + \eta\frac{W}{A} \quad . \tag{6}$$

We now introduce dimensionless charge densities and work per unit area:

$$\Sigma_0 = \frac{\sigma_0}{\sqrt{k\kappa}} \; ; \; \Sigma_s = \frac{\sigma_s}{\sqrt{k\kappa}} \tag{7}$$

$$\omega = \frac{1}{k}\frac{W}{A} \quad . \tag{8}$$

In terms of these, Eq. (6) becomes

$$\Sigma_s{}^2 = \Sigma_0{}^2 + 2\eta\omega \quad , \tag{9}$$

or in differential form,

$$d\Sigma_s = \frac{2\eta}{\sqrt{\Sigma_0{}^2 + 2\eta\omega}}\, d\omega \quad . \tag{10}$$

We make a simplification at this point by again treating the contact force as if it were constant over the contact region. In that case, the dimensionless work per unit area, done by friction in a interval $d\tau$, is:

$$\frac{d\omega}{d\tau_c} = \frac{\mu\delta}{2S_c}\left[\frac{dX_0}{d\tau} + \rho\sin(\phi+\theta)\frac{d\phi}{d\tau}\right] \quad . \tag{11}$$

Finally, it seems unrealistic to expect the saturation charge density to remain permanently elevated as a result of work done by friction. We therefore assume that it will tend to relax to its static contact value over a characteristic dimensionless time τ_r. Eq. (10) now becomes

$$d\Sigma_s = \left[\frac{2\eta}{\sqrt{\Sigma_0{}^2 + 2\eta\omega}}\frac{d\omega}{d\tau} + \frac{1}{\tau_r}(\Sigma_0 - \Sigma_s)\right] d\tau_c \quad . \tag{12}$$

The relaxation or 'back-flow' term is the second term inside the square brackets. The charge transfer is governed by the following modified dimensionless form of Eq. (2):

$$\frac{d\Sigma}{d\tau_c} = \frac{1}{\tau_0}(\Sigma_s - \Sigma) \quad . \tag{13}$$

For simplicity, τ_r is set equal to τ_0 in all of the following simulations. The net particle charge is expressed in terms of the static saturation charge density and the total particle surface area, i.e. $Q/(\sigma_0.A_s)$. This dimensionless composite variable reaches a value of

one when the entire available particle surface has the 'static' saturation charge density σ_0. Under the static charge transfer model, this dimensionless charge cannot increase beyond unity; it can, however, under the sliding charge transfer model. It should also be noted that the static charge transfer model does not allow for back-flow of charge, and hence the dimensionless particle charge cannot decrease with time under this model. The sliding contact charging model, on the other hand, incorporates a relaxation mechanism, and is not subject to this restriction.

III. RESULTS AND DISCUSSION

The variables that determine the particle motion were listed in the previous section. The initial position and velocity of the particle are also critical in this regard. The particle charge depends on the particle motion, and also on dimensionless charging time τ_0 (for the simple static contact model) and on τ_0, Σ_0 and η (for the sliding contact model). It is well beyond the scope of this paper to examine the influence of all of these variables on the charging behaviour. Instead, a few representative cases have been chosen to illustrate the effect of the particle roundness ratio.

The initial dynamic conditions were identical for all simulations; the particle's long axis was aligned parallel to the surface and the rotational velocity was zero. The particle was assumed to have dropped straight down onto the plate with dimensionless velocity 0.025. For $\beta = 45°$, this meant that the initial velocity had equal components normal and tangential to the surface. In all cases, $\tau_0 = 1.0$. For those simulations that included sliding charge augmentation, $\Sigma_0 = 0.01$ and $\eta = 0.1$. The coefficients μ and ν were set equal, and given one of two values; 0.1 for the 'low friction' case, and 1.0 for the 'high friction' case. In the latter case, the friction coefficient was just short of the critical value that would prevent sliding if the particle were merely placed on the surface.

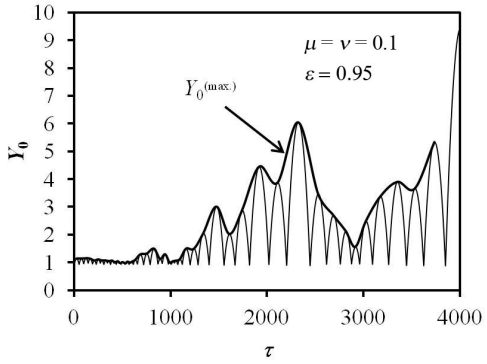

Fig. 3. The bouncing amplitude $Y_0^{(\max.)}$ is obtained by taking the upper envelope of the normal particle-plate distance, Y_0.

To illustrate the particle motion, the normal distance of the particle centre above the plate (Y_0) is plotted as a time series. Figure 3 shows an example, this one for the low friction case and $\varepsilon = 0.95$. In this case, the particle bounces off the surface with varying amplitude. For comparison between different simulations, the upper envelope of these bounces is used ($Y_0^{(\max.)}$, as shown in Figure 3). In Figure 4, time series of the bounce amplitude are shown for various values of the roundness ratio and for low and high friction.

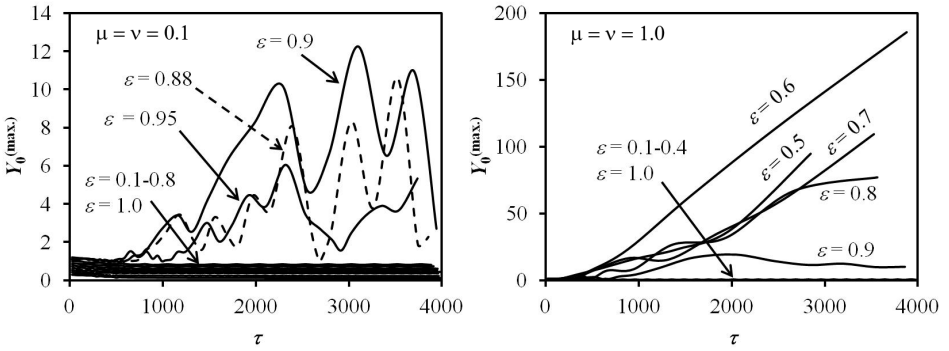

Fig. 4. Bounce amplitude vs. dimensionless time, for low friction (left) and high friction (right) cases. For $\varepsilon = 0.1-0.4$ and $\varepsilon = 1.0$, $Y_0^{(\max.)} \approx 1$.

Several important trends are evident. For both low and high friction, the particle tends to stay very close to the surface for low values of the roundness ratio (i.e. highly flattened particles). There is then a very sharp transition to large-amplitude bouncing at a particular value of ε: at around $\varepsilon = 0.88$ for the low friction case and approximately $\varepsilon = 0.45$ for the high friction case. We denote this transitional roundness ratio ε_t. As the roundness ratio increases from this transition, the bouncing amplitude rises further, peaks, and falls away again to a very low value at $\varepsilon = 1$ (a perfectly round particle). While some of the plots show the bouncing amplitude increasing monotonically with time (e.g. $\varepsilon = 0.6$ in the high-friction case), it should eventually reach a more-or-less stable state, where rate of gain in kinetic energy from gravity is balanced by energy losses due to friction (e.g. $\varepsilon = 0.9$ in the high-friction case). In both low and high friction cases, the sharp transition in behaviour occurs between those particles that maintain a quasi-fixed orientation ('sliding') and those that are able to full rotate in the ϕ-direction ('rolling' or 'tumbling'). The orientation of the sliding particles is described as 'quasi-fixed') because they adopt a rocking motion, rather than a genuinely fixed orientation. Nonetheless, in these cases, a large proportion of the particle surface never comes into contact with the plate, with important consequences for charge transfer (see shortly). The critical roundness ratio ε_t is lower in the high friction case than in the low friction case, because larger tangential forces can be developed at the interface, leading to a larger rolling torque on the particle.

Apart from particles that are very nearly round ($\varepsilon \to 1$), rolling inevitably turns into tumbling, as the particle 'kicks' against the surface and is catapulted away from the surface. A final mode of particle behaviour can be best seen in Figure 4, for the low friction case. Here, where $\tau < 1000$, evidence of bouncing with a quasi-fixed orientation can be observed. This mode would probably be far more pronounced if the angle of the incident velocity to the surface were more oblique (i.e., more of a 'skimming' incidence). It may appear at first that the bouncing amplitude is much larger in the high friction case than the low friction case; however, for the same roundness ratio, the difference is not particularly great (e.g., $\varepsilon = 0.9$). In the low friction case, tumbling does not occur at those roundness ratios for which the amplitude is greatest in the high-friction case.

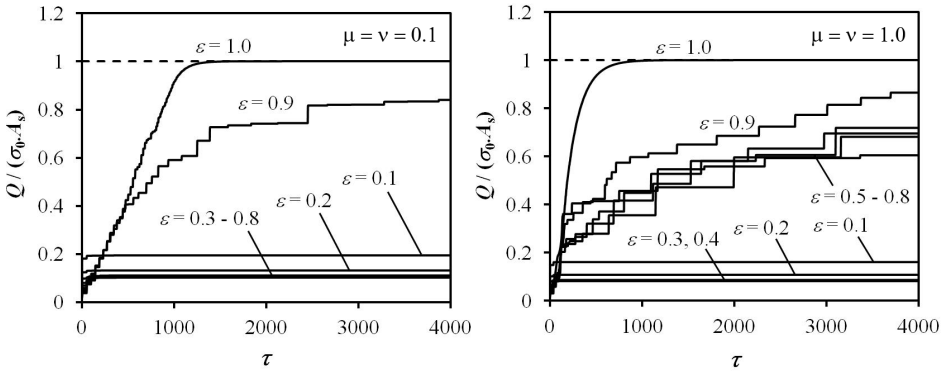

Fig. 5. Dimensionless charge vs. dimensionless time, for low friction (left) and high friction (right) cases. Charge calculated using the static capacitive charging model.

Having noted some key trends in the particle motion, we now proceed to examine their effect on the charge transfer. We begin with the simple static charging model. Figure 5 shows time series of the particle charge for various roundness ratios in the low and high friction regimes. In Figure 6, the same data are plotted against the roundness ratio at five different time values. We see an immediate correspondence between these data and those in Figure 4. For small roundness ratios ($\varepsilon < \varepsilon_t$), the dimensionless charge approaches a limiting value with time that is substantially less than unity. This value actually decreases with roundness ratio. The radius of curvature of the part of the particle in contact with the surface, and thus the contact area, becomes smaller with increasing roundness ratio; thus , the maximum charge attainable also decreases. As the roundness ratio decreases to zero (i.e. the particle becomes completely flattened), the contact area as a fraction of the total area, and thus the maximum dimensionless charge, should approach 0.5. As ε increases past ε_t , and begins to roll or tumble, the charge time-series abruptly change, and begin to approach a maximum value of unity, since the entire particle surface is now available for charging. This rapid transition is best observed in Figure 6. For the lower roundness ratios

in this regime, the charge tends to increase in a series of discontinuous jumps, corresponding to collisions with the surface, and the transient large contact areas associated with them. As the roundness ratio approaches one, these jumps become smaller. Eventually, for a completely round particle, the only jumps observed are those arising from the initial normal velocity; as already noted, these decay over $\tau \approx 0 \rightarrow 1000$. This corresponds with the observed trend in bouncing amplitude with roundness ratio. Importantly, however, the charge increases more rapidly to unity as the roundness ratio increases. This is precisely because 'rolling' particles (e.g., $\varepsilon = 1$) spend a higher proportion of their time in contact with the surface, and exchanging charge, than violently tumbling particles (e.g., $\varepsilon = 0.5$ in the high friction case).

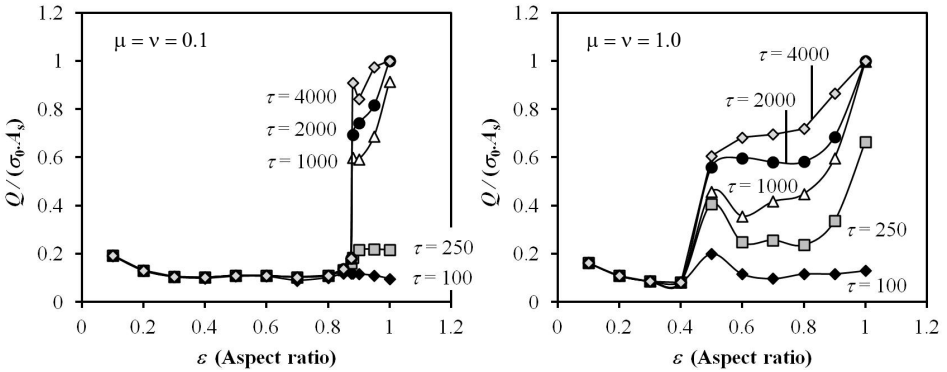

Fig. 6. Dimensionless charge vs. roundness ratio, for low friction (left) and high friction (right) cases, at various times. Charge calculated using the static capacitive charging model.

Figures 7 and 8 show equivalent data for the sliding charge model. Note that the charge is still expressed as a fraction of the saturated static charge density multiplied by the total area. Since in our model the dynamic saturation charge density can be augmented by frictional work at the interface, the dimensionless charge can exceed unity, and can decrease with time due to charge back-flow. For $\varepsilon < \varepsilon_t$, as in the static charging case, the dimensionless charge approaches a relatively small constant value. As ε exceeds ε_t, the dimensionless charge increases well beyond unity in a series of large jumps, again corresponding to collisions with the surface. In contrast to the static charging model, for $\tau \geq 2000$, the charge actually decreases with roundness ratio. For $\varepsilon = 1$, in both the low and high friction regimes, the charge increases to a maximum at $\tau \sim 1000$, then decreases slightly to a stable value thereafter. It is possible that the charge on lower roundness ratio particles will stabilise to a lesser value at a later time, but there is no sign of it in the interval studied. The trends in the charge data can again be explained readily in terms of the particle dynamics. For $\varepsilon < \varepsilon_t$, the particle slides, but the contact is relatively gentle, particularly in the low friction case, as there are few if any violent collisions. In the high fric-

tion case, the interfacial force is somewhat larger, but the sliding speed is slower. In both friction regimes, for $\varepsilon < \varepsilon_t$, little work is done at the interface to elevate the saturation charge density. Since contact is for the most part continuous, charge back-flow is therefore also continuous. As before, the area of the particle surface able to make contact with the surface is limited.

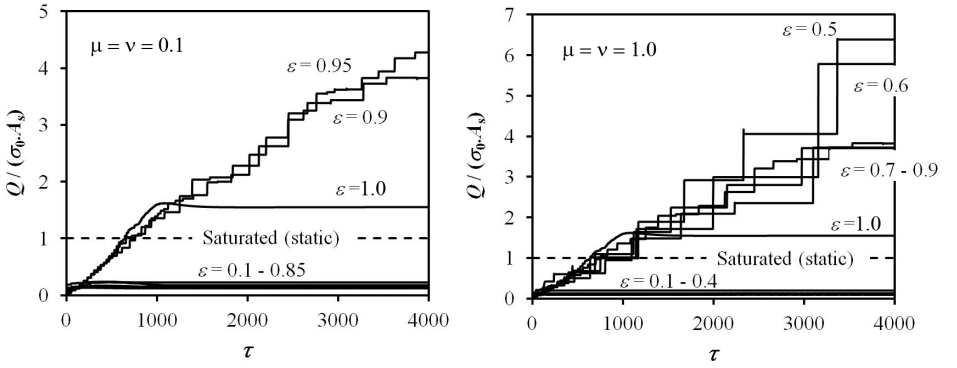

Fig. 7. Dimensionless charge vs. dimensionless time, for low friction (left) and high friction (right) cases. Charge calculated using the sliding contact charging model.

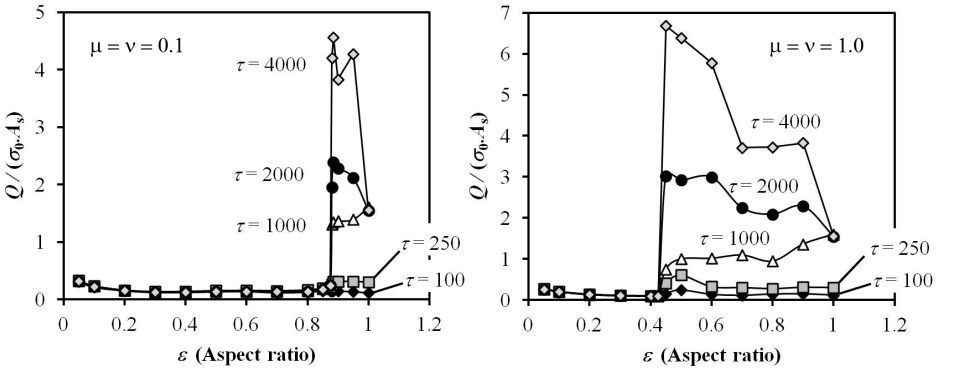

Fig. 8. Dimensionless charge vs. roundness ratio, for low friction (left) and high friction (right) cases, at various times. Charge calculated using the sliding contact charging model.

For roundness ratios approaching unity, the entire particle surface is available for contact, and the limiting charge is therefore larger. However, as for low roundness ratios, frictional forces at the interface tend to be small, for the reasons already outlined, and also be-

cause the particle will tend to roll. Again, the particle is in continuous contact with the surface, and continuous saturation charge relaxation occurs.

In contrast, for roundness ratios just exceeding ε_t, the particle tends to tumble, leading to large transient interfacial forces, large transient contact areas and high collision speeds. Contact is discontinuous, but this has the competing effects of limiting saturation charge relaxation and charge transfer. The result is that the dimensionless charge increases to a number of times the static saturation value of unity.

IV. Conclusions and Future work

Previous experimental studies have reinforced the importance of particle shape to particle-surface tribocharging. The aim of this work was therefore to begin to understand the mechanisms behind this influence. We have developed a simple two-dimensional model of the charging of an elliptical particle on a tilted flat surface. This model incorporates a very simple static capacitive charging mechanism and a sliding contact charging mechanism based on the frictional work done at the interface, with a relaxation term for charge back-flow. This latter charging mechanism was selected as the most tractable physically plausible option, not because it is supported by any physical evidence. It should therefore be regarded as provisional, until a better alternative becomes available. The overall model should be treated with similar caution. At this early stage, its usefulness is in providing broad insights rather than quantitative predictions.

For the very limited set of conditions explored in this paper, some clear trends in the charging behavior with particle roundness ratio were apparent. Particles with a low roundness ratio (i.e. highly-flattened particles) tend to slide with a quasi-fixed orientation, i.e., they rock back and forth as they slide, but do not actually roll or tumble. At a certain specific roundness ratio, which is lower for high-friction contact than low-friction contact, the particle begins to roll. Unless the roundness ratio is very close to unity, this invariably leads to violent tumbling and bouncing. For the simple capacitive charging model, in the sliding (low roundness ratio) regime, the dimensionless charge approaches a value substantially less than one, and decreases with increasing roundness ratio, since only a limited section of the surface is available for contact, and this decreases with the radius of curvature. When the roundness ratio exceeds the critical value and the orientation is no longer quasi-fixed, the entire particle surface becomes available for charging, and the dimensionless charge approaches one. The rate of approach to this maximum value increases with roundness ratio, as the tumbling/bouncing contact mode of the more irregular particles becomes continuous rolling, and the proportion of the total time spent in contact with the surface increases.

For our frictional work model of sliding contact charging, the trend for sliding contact with quasi-fixed orientation is similar to that above. However, for rolling and tumbling contact, the trend is quite different, at least for the parameters chosen here. In this regime, a relatively irregular particle that undergoes violent tumbling obtains a larger charge than a round particle that rolls. For these particular cases, the much larger transient interfacial forces during tumbling, and the large (albeit intermittent) work done, are more important to charging that the continuity of contact offered by rolling.

As we have already emphasised, a large part of the parameter space delineated by our model has not been explored at all. Apart from the provisional nature of the sliding contact model, the effect of varying the surface elasticity, charging time coefficient, ratio of normal to tangential force (i.e., tilt angle) and initial particle orientation remain to be studied. The initial velocity vector is particularly important for the study of tribocharging devices, since it will typically be a key adjustable parameter during operations. These parameters will all be explored in future work.

ACKNOWLEDGEMENTS

Dr. Ireland is the recipient of an Australian Research Council Future Fellowship (project number FT110100295).

APPENDIX

Auxiliary quantities associated with the elliptical particle geometry:

$$\tan\phi\tan\theta = \frac{b^2}{a^2} \tag{14}$$

$$\tan\phi\tan\alpha = \frac{b}{a} \tag{15}$$

$$r = \frac{a\,b}{\sqrt{\left(a\sin\theta\right)^2 + \left(b\cos\theta\right)^2}} \tag{16}$$

$$r_{\mathrm{c}} = \frac{\left[\left(a\sin\alpha\right)^2 + \left(b\cos\alpha\right)^2\right]^{3/2}}{a\,b} \tag{17}$$

Normal indentation distance:

$$d_{\mathrm{y}} = \begin{cases} r\sin\left(\phi+\theta\right) - y_0 & \text{if} \quad r\sin\left(\phi+\theta\right) \geq y_0 \\ 0 & \text{if} \quad r\sin\left(\phi+\theta\right) < y_0 \end{cases} \tag{18}$$

Tangential compliance:

$$\frac{\mathrm{d}d_{\mathrm{x}}}{\mathrm{d}t} = \frac{\mathrm{d}x_0}{\mathrm{d}t} - r_{\mathrm{c}} \frac{\mathrm{d}\phi}{\mathrm{d}t} \tag{19}$$

In our solution algorithm, d_{x} is reset to zero whenever the particle regains contact with the surface after losing contact. It is reset to $\mu F_{\mathrm{c}}^{\mathrm{N}} / k$ whenever $\left| F_{\mathrm{c}}^{\mathrm{T}} \right|$ falls below $\mu F_{\mathrm{c}}^{\mathrm{N}}$ (i.e., when re-stick occurs).

Contact force components:

$$F_{\mathrm{c}}^{\mathrm{T}} = \begin{cases} -kd_{\mathrm{x}} & \text{if} \quad d_{\mathrm{y}} > 0 \quad \text{and} \quad k\left|d_{\mathrm{x}}\right| \le \mu F_{\mathrm{c}}^{\mathrm{N}} \\ \text{-sign}\left[\dfrac{dx_0}{dt} + r\sin\left(\phi+\theta\right)\dfrac{d\phi}{dt}\right]\mu F_{\mathrm{c}}^{\mathrm{N}} & \text{if} \quad d_{\mathrm{y}} > 0 \quad \text{and} \quad k\left|d_{\mathrm{x}}\right| > \mu F_{\mathrm{c}}^{\mathrm{N}} \\ 0 & \text{if} \quad d_{\mathrm{y}} \le 0 \end{cases} \tag{20}$$

$$F_{\mathrm{c}}^{\mathrm{N}} = \begin{cases} kd_{\mathrm{y}}\left(1 - \text{sign}\left[\dfrac{\mathrm{d}y_0}{dt}\right]\nu\right) & \text{if} \quad d_{\mathrm{y}} > 0 \\ 0 & \text{if} \quad d_{\mathrm{y}} \le 0 \end{cases} \tag{21}$$

Two-dimensional rigid body equations of motion, for an elliptical particle:

$$m\frac{d^2x_0}{dt^2} = F_0^{\mathrm{T}} + F_{\mathrm{c}}^{\mathrm{T}} \tag{22}$$

$$m\frac{d^2y_0}{dt^2} = F_0^{\mathrm{N}} + F_{\mathrm{c}}^{\mathrm{N}} \tag{23}$$

$$\frac{m}{4}\left(a^2+b^2\right)\frac{d^2\phi}{dt^2} = F_{\mathrm{c}}^{\mathrm{T}}\sin\left(\phi+\theta\right)r - F_{\mathrm{c}}^{\mathrm{N}}\cos\left(\phi+\theta\right)r \tag{24}$$

Dimensionless forms of Eqs. (20-24):

$$\Psi_{\mathrm{c}}^{\mathrm{T}} = \begin{cases} -\delta_{\mathrm{x}} & \text{if} \quad \delta_{\mathrm{y}} > 0 \quad \text{and} \quad \left|\delta_{\mathrm{x}}\right| \le \mu \Psi_{\mathrm{c}}^{\mathrm{N}} \\ -\mathrm{sign}\left[\dfrac{dX_0}{d\tau} + \rho \sin\left(\phi+\theta\right)\dfrac{d\phi}{d\tau}\right]\mu\,\Psi_{\mathrm{c}}^{\mathrm{N}} & \text{if} \quad \delta_{\mathrm{y}} > 0 \quad \text{and} \quad \left|\delta_{\mathrm{x}}\right| > \mu \Psi_{\mathrm{c}}^{\mathrm{N}} \\ 0 & \text{if} \quad \delta_{\mathrm{y}} \le 0 \end{cases} \tag{25}$$

$$\Psi_{\mathrm{c}}^{\mathrm{N}} = \begin{cases} \delta_{\mathrm{y}}\left(1 - \mathrm{sign}\left[\dfrac{\mathrm{d}Y_0}{d\tau}\right]\nu\right) & \text{if} \quad \delta_{\mathrm{y}} > 0 \\ 0 & \text{if} \quad \delta_{\mathrm{y}} \le 0 \end{cases} \tag{26}$$

$$\frac{d^2 X_0}{d\tau^2} = \Gamma \sin\beta + \Psi_{\mathrm{c}}^{\mathrm{T}} \tag{27}$$

$$\frac{d^2 Y_0}{d\tau^2} = -\Gamma \cos\beta + \Psi_{\mathrm{c}}^{\mathrm{N}} \tag{28}$$

$$\frac{1}{4}\left(1+\varepsilon^2\right)\frac{d^2\phi}{d\tau^2} = \Psi_{\mathrm{c}}^{\mathrm{T}} \sin\left(\phi+\theta\right)\rho - \Psi_{\mathrm{c}}^{\mathrm{N}} \cos\left(\phi+\theta\right)\rho \tag{29}$$

REFERENCES

[1] T. B. Jones and J. L. King, *Powder Handling and Electrostatics: Understanding and Preventing Hazard*: Lewis Publishers, 1991.

[2] A. G. Bailey, "Charging of Solids and Powders," *Journal of Electrostatics,* vol. 30, pp. 167-180, May 1993.

[3] J. R. Mountain, M. K. Mazumder, R. A. Sims, D. L. Wankum, T. Chasser, and P. H. Pettit, "Triboelectric charging of polymer powders in fluidization and transport processes," *Ieee Transactions on Industry Applications,* vol. 37, pp. 778-784, May-Jun 2001.

[4] F. J. Wang, J. X. Zhu, and J. M. Beeckmans, "Pressure gradient and particle adhesion in the pneumatic transport of cohesive fine powders," *International Journal of Multiphase Flow,* vol. 26, pp. 245-265, Feb 2000.

[5] J. A. Cross, H. Mumfordvanurk, and S. Singh, "Some Experiments in Powder Charging and Its Significance to Industrial-Processes," *Journal of Electrostatics,* vol. 10, pp. 235-235, 1981.

[6] G. E. Klinzing, "Clustering under the Influence of Electrostatic Forces," *International Journal of Multiphase Flow,* vol. 12, pp. 853-857, Sep-Oct 1986.

[7] M. Glor, "Ignition hazard due to static electricity in particulate processes," *Powder Technology,* vol. 135-136, pp. 223-233, 2003.

[8] L. B. Schein, "Recent advances in our understanding of toner charging," *Journal of Electrostatics,* vol. 46, pp. 29-36, 1999.

[9] S. Trigwell, K. B. Tennal, M. K. Mazumder, and D. A. Lindquist, "Precombustion cleaning of coal by triboelectric separation of minerals," *Particulate Science and Technology,* vol. 21, pp. 353-364, Oct-Dec 2003.

[10] J. Wei and M. J. Realff, "Design and optimization of free-fall electrostatic separators for plastics recycling," *Aiche Journal,* vol. 49, pp. 3138-3149, Dec 2003.

[11] J. K. Kim, H. C. Cho, S. C. Kim, and H. S. Chun, "Electrostatic beneficiation of fly ash using an ejector-tribocharger," *Journal of Environmental Science and Health Part a-Toxic/Hazardous Substances & Environmental Engineering,* vol. 35, pp. 357-377, 2000.

[12] R. K. Dwari and K. H. Rao, "Fine coal preparation using novel tribo-electrostatic separator," *Minerals Engineering,* vol. 22, pp. 119-127, Jan 2009.

[13] M. J. Pearse and M. I. Pope, "Triboelectric separation of quartz-calcite and quartz-apatite powders after chemical conditioning," *Powder Technology,* vol. 17, pp. 83-89, 1977.

[14] P. Mehrani, H. T. T. Bi, and J. R. Grace, "Bench-scale tests to determine mechanisms of charge generation due to particle-particle and particle-wall contact in binary systems of fine and coarse particles," *Powder Technology,* vol. 173, pp. 73-81, Apr 2007.

[15] T. Matsuyama and H. Yamamoto, "Characterizing the electrostatic charging of polymer particles by impact charging experiments," *Advanced Powder Technology,* vol. 6, pp. 211-220, 1995.

[16] T. Matsuyama and H. Yamamoto, "Charge relaxation process dominates contact charging of a particle in atmospheric conditions," *Journal of Physics D-Applied Physics,* vol. 28, pp. 2418-2423, Dec 1995.

[17] T. Matsuyama and H. Yamamoto, "Charge-relaxation process dominates contact charging of a particle in atmospheric condition .2. The general model," *Journal of Physics D-Applied Physics,* vol. 30, pp. 2170-2175, Aug 1997.

[18] S. Matsusaka, M. Oki, and H. Masuda, "Control of electrostatic charge on particles by impact charging," *Advanced Powder Technology,* vol. 18, pp. 229-244, Mar 2007.

[19] S. Matsusaka, H. Maruyama, T. Matsuyama, and M. Ghadiri, "Triboelectric charging of powders: A review," *Chemical Engineering Science,* vol. 65, pp. 5781-5807, Nov 2010.

[20] H. Watanabe, M. Ghadiri, T. Matsuyama, Y. L. Ding, K. G. Pitt, H. Maruyama, S. Matsusaka, and H. Masuda, "Triboelectrification of pharmaceutical powders by particle impact," *International Journal of Pharmaceutics,* vol. 334, pp. 149-155, Apr 2007.

[21] P. M. Ireland, "Triboelectrification of particulate flows on surfaces: Part I - Experiments," *Powder Technology,* vol. 198, pp. 189-198, Mar 2010.

[22] P. M. Ireland, "Triboelectrification of particulate flows on surfaces: Part II - Mechanisms and models," *Powder Technology,* vol. 198, pp. 199-210, Mar 2010.

[23] D. K. Yanar and B. A. Kwetkus, "Electrostatic separation of polymer powders," *Journal of Electrostatics,* vol. 35, pp. 257-266, Aug 1995.

[24] K. Nicholson, P. M. Ireland, E. Wanless, and G. J. Jameson, "Design and construction of a laboratory-scale cyclone tribocharger," in *Proceedings of Chemeca* Newcastle, 2008, p. 241.

[25] P. Ireland and G. J. Jameson, "Particle mechanics and the design of cyclone tribochargers," in *Proceedings of the XXV Mineral Processing Conference (IMPC)*, Brisbane 2010, pp. 833-842.

[26] P. M. Ireland and K. Nicholson, "Analysis and comparison of particle tribochargers," *Minerals Engineering,* vol. 24, pp. 914-922, Jul 2011.

[27] V. L. Popov, *Contact Mechanic and Friction: Physical Principles and Applications*, 2010.

[28] J. Lowell and A. C. Roseinnes, "Contact Electrification," *Advances in Physics,* vol. 29, pp. 947-1023, 1980.

[29] J. Dyson and W. Hirst, "The true contact area between solids," *Proceedings of the Royal Society of London,* vol. 67, p. 309, 1954.

[30] I. I. Inculet and E. P. Wituschek, "Electrification by friction in a 3 x 10^{-7} Torr vacuum," in *Static Electrification (Institute of Physics Conference Series No.4)* London: Taylor and Francis, 1967, pp. 37-43.

[31] F. P. Bowden and D. Tabor, *The Friction and Lubrication of Solids: I*. Oxford: Clarendon, 1954.

[32] P. M. Ireland, "The role of changing contact in sliding triboelectrification," *Journal of Physics D-Applied Physics,* vol. 41, Jan 2008.

[33] A. Wahlin and Backstro.G, "Sliding electrification of Teflon by metals," *Journal of Applied Physics,* vol. 45, pp. 2058-2064, 1974.

[34] J. Lowell, "Electrification of polymers by metals," *Journal of Physics D-Applied Physics,* vol. 9, pp. 1571-1585, 1976.